Estimating wetland methane emissions from the northern high latitudes from 1990 to 2009 using artificial neural networks

Xudong Zhu,[1] Qianlai Zhuang,[1] Zhangcai Qin,[1] Mikhail Glagolev,[2] and Lulu Song [1,3,4]

Received 24 April 2012; revised 9 April 2013; accepted 26 May 2013.

[1] Methane (CH_4) emissions from wetland ecosystems in nothern high latitudes provide a potentially positive feedback to global climate warming. Large uncertainties still remain in estimating wetland CH_4 emisions at regional scales. Here we develop a statistical model of CH_4 emissions using an artificial neural network (ANN) approach and field observations of CH_4 fluxes. Six explanatory variables (air temperature, precipitation, water table depth, soil organic carbon, soil total porosity, and soil pH) are included in the development of ANN models, which are then extrapolated to the northern high latitudes to estimate monthly CH_4 emissions from 1990 to 2009. We estimate that the annual wetland CH_4 source from the northern high latitudes (north of 45°N) is 48.7 Tg CH_4 yr^{-1} (1 Tg = 10^{12} g) with an uncertainty range of 44.0~53.7 Tg CH_4 yr^{-1}. The estimated wetland CH_4 emissions show a large spatial variability over the northern high latitudes, due to variations in hydrology, climate, and soil conditions. Significant interannual and seasonal variations of wetland CH_4 emissions exist in the past 2 decades, and the emissions in this period are most sensitive to variations in water table position. To improve future assessment of wetland CH_4 dynamics in this region, research priorities should be directed to better characterizing hydrological processes of wetlands, including temporal dynamics of water table position and spatial dynamics of wetland areas.

Citation: Zhu, X., Q. Zhuang, Z. Qin, M. Glagolev, and L. Song (2013), Estimating wetland methane emissions from the northern high latitudes from 1990 to 2009 using artificial neural networks, *Global Biogeochem. Cycles*, *27*, doi:10.1002/gbc.20052.

1. Introduction

[2] Methane (CH_4) is the second most significant greenhouse gas after carbon dioxide (CO_2). According to the latest Intergovernmental Panel on Climate Change report, the radiative efficiency of CH_4 is about 25 times that of CO_2 on a 100 year time horizon [*Solomon et al*., 2007]. The atmospheric concentration of CH_4 has increased from a preindustrial value of about 700 ppb to a current value of about 1790 ppb [*Dlugokencky et al*., 2009], contributing 0.48 W m^{-2} [*O'Connor et al*., 2010] of radiative forcing to the atmosphere. Global CH_4 budget can be relatively well determined based on observations of atmospheric concentration of CH_4. However, the high spatial and temporal variability of CH_4 makes it hard to fully understand the strength and trends of natural and anthropogenic contributing sources [*Solomon et al*., 2007]. Among these multiple sources, wetlands are thought to be the single largest and climate-dominated natural source [*Bartlett and Harriss*, 1993; *Wuebbles and Hayhoe*, 2002]. And it was estimated that more than half of global wetlands are located in the northern high latitudes above 50°N [*Aselmann and Crutzen*, 1989].

[3] The amount of CH_4 emitted from wetland soils is determined by the balance between CH_4 production and consumption. In anoxic environments, e.g., saturated soils below the water table, CH_4 is produced by methanogens which require oxygen-free environments [*Whitman et al*., 1992]. In aerobic environments, e.g., unsaturated soils above the water table, CH_4 is oxidized by methanotrophic bacteria in the presence of oxygen [*Hanson and Hanson*, 1996]. Both of CH_4 production and oxidation are mainly controlled by soil temperature, pH, and substrate availability [*Christensen et al*., 1995; *MacDonald et al*., 1998; *Wagner et al*., 2005]. CH_4 can escape to the atmosphere via diffusion, plant-mediated transport, and ebullition, and the sum of these three release pathways represents the total amount of CH_4 emitted to the atmosphere from the soil.

[4] Estimates of wetland CH_4 emissions are often obtained using "bottom-up" approaches, ranging from simple empirical or statistical models [e.g., *Andronova and Karol*, 1993; *Granberg et al*., 1997; *Levy et al*., 2011] to detailed process-based models [e.g., *Cao et al*., 1996; *Walter et al*., 2001; *Zhuang et al*., 2004]. Previous process-based model simulations presented a large uncertainty in the estimates of

Additional supporting information may be found in the online version of this article.

[1]Department of Earth, Atmospheric, and Planetary Sciences, Purdue University, West Lafayette, Indiana, USA.
[2]Department of Physics and Melioration of Soils, Moscow State University, Moscow, Russia.
[3]Institute of Geographic Sciences and Natural Resources Research, Chinese Academy of Sciences, Beijing, China.
[4]College of Resources and Environment, Graduate University of the Chinese Academy of Sciences, Beijing, China.

Corresponding author: X. Zhu, Department of Earth, Atmospheric, and Planetary Sciences, Purdue University, West Lafayette, IN 47907, USA. (zhu123@purdue.edu)

0886-6236/13/10.1002/gbc.20052

Table 1. Description of the Sites Used in This Analysis

ID	Site Name	N	Ecosystem	Longitude (°)	Latitude (°)	Temperature (°C)	Precipitation (mm month^{-1})	Water Table Depth (cm)	Carbon Content (%)	Total Porosity (%)	pH	CH_4 Fluxes (g CH_4 m^{-2} month^{-1})	Reference
1	Toolik Lake, Alaska, USA	8	Upland tundra	−149.5	68.5	8.40	34.37	−13.50 to 14.10	3.56	50.08	4.50–5.40	0.02–1.28	*Christensen* [1993]
2	Toolik Lake, Alaska, USA	16	Wet meadow tundra	−149.5	68.5	8.40–13.10	34.37–41.15	−11.80 to 5.70	3.56	50.08	4.50–6.50	0.68–3.37	*Christensen* [1993]
3	Patuanak, Saskatchewan, Canada	21	Frost mound	−107.5	56.0	16.60–20.00	43.69	−46.70 to −16.30	6.43	49.40	4.63	0.00–0.01	*Turetsky et al.* [2002]
4	Yamal Peninsula, Russia	14	Treeless subarctic tundra	71.5	68.0	12.50–22.00	61.33	−20.00 to 7.00	6.19	50.70	6.11	0.13–5.86	*Heyer et al.* [2002]
5	Chersky, Russia	10	Tundra-taiga transition	161.5	69.0	11.60	35.05	−15.00 to 12.00	6.81	53.20	5.70	−0.02–8.43	*Nakano et al.* [2000]
6	Lena Delta, Russia	15	Wet polygonal tundra	126.5	72.5	7.00	46.60	−12.00 to 3.00	4.27	28.93	3.32	0.23–2.82	*Sachs et al.* [2010]
7	Thompson, Manitoba, Canada	15	Collapse bog	−98.0	55.5	15.40	59.43	−9.00 to −1.00	20.73	79.10	4.00–6.80	0.59–6.78	*Bellisario et al.* [1999]
8	North Point-Kinosheo transect, Hudson Bay Lowlands, Canada	85	Coastal fen	−80.5	51.5	10.80	83.63	−18.00 to −1.00	9.08	57.43	5.00	0.03–0.49	*Moore et al.* [1994]
9	North Point-Kinosheo transect, Hudson Bay Lowlands, Canada	85	Bog	−82.0	51.5	10.80	80.20	−21.00 to 5.00	33.86	88.56	4.85	0.08–3.14	*Moore et al.* [1994]
10	Lementa Bog, Fairbanks, Alaska, USA	18	Bog	−147.5	65.0	16.00	37.13	−40.00 to −20.00	7.39	59.20	3.94–4.74	0.00–1.72	*Moosavi et al.* [1996]
11	Prudhoe Bay, Alaska, USA	28	Wet coastal tundra	−148.5	70.5	6.50	23.02	−5.00 to 0	1.39	24.82	3.20	2.05–3.65	*Vourlitis et al.* [1993]
12	Prudhoe Bay, Alaska, USA	28	Wet coastal tundra	−148.5	70.0	10.00	36.35	0 to 5.00	9.08	55.30	5.89	5.00–6.10	*Vourlitis et al.* [1993]
13	Barrow, Alaska, USA	8	Wet/moist coastal tundra	−157.0	71.0	5.00	26.00	−15.00 to 5.00	2.56	45.68	5.89	0.30–2.01	*Rhew et al.* [2007]
14	Tobolsk, West Siberia, Russia	12	Ombrotrophic hollow/poor fen	68.0	58.5	11.05–14.72	83.80–97.70	2.00 to 45.00	2.11–9.89	50.74–58.53	4.18–4.58	−0.08–3.45	*Glagolev et al.* [2011]
15	Surgut, West Siberia, Russia	15	Oligotrophic bog	73.5	61.5	12.10–21.70	101.30	−6.00 to 50.00	9.85	62.78	3.82–4.61	−0.03–1.50	*Glagolev et al.* [2011]
16	Pangody, West Siberia, Russia	16	Palsa/hollow	75.0	66.0	9.64–15.47	40.10–42.00	−3.00 to 35.00	5.75–10.59	57.32–64.46	4.48–5.30	−0.04–1.24	*Glagolev et al.* [2011]
17	Plotnikovo, West Siberia, Russia	116	Bog/fen	83.0	57.0	8.75–44.64	25.90–108.60	−17.00 to 40.00	13.19–18.31	62.11–67.32	2.31–5.80	−0.27–8.70	*Glagolev et al.* [2011]
18	Noyabrsk Hills, West Siberia, Russia	22	Bog/peat mat/pool/palsa	74.5	63.0	14.40–21.01	97.70	−18.00 to 45.00	26.70	88.97	4.14–4.68	0.00–3.32	*Glagolev et al.* [2011]
19	Noyabrsk Palsa, West Siberia, Russia	12	Palsa/hollow	75.5	64.0	11.95–13.72	87.10	−11.00 to 30.00	10.60	64.88	4.20–4.72	−0.02–6.52	*Glagolev et al.* [2011]
20	Vah, West Siberia, Russia	12	Moss	70.5	59.5	1.14–13.48	34.90	−15.00 to 20.00	3.71	50.68	6.80–7.03	0.62–7.39	*Glagolev et al.* [2011]
21	Muhrino, West Siberia, Russia	243	Bog/waterlogged forest/mire/lake	68.5	61.0	4.00–41.14	27.20–83.80	−10.00 to 95.00	26.66	88.44	3.31–5.30	−0.22–7.93	*Glagolev et al.* [2011]
22	Tazovsky, West Siberia, Russia	72	Lake/mire/bog/fen/moss	79.0	67.0	7.33–19.00	42.30	−25.00 to 20.00	1.59	50.34	4.55–5.71	−0.03–5.33	*Glagolev et al.* [2011]
23		59		78.5	71.0	4.00–14.07	45.60		15.82	60.01		0.14–2.10	

Table 1. (continued)

ID	Site Name	N	Ecosystem	Longitude (°)	Latitude (°)	Temperature (°C)	Precipitation (mm month^{-1})	Water Table Depth (cm)	Carbon Content (%)	Total Porosity (%)	pH	CH_4 Fluxes (g CH_4 m^{-2} month^{-1})	Reference
	Gyda, West Siberia, Russia		Dwarf shrubs/ lake/fen					−4.00 to 17.00			5.75–6.26		*Glagolev et al.* [2011]
24	Skala, West Siberia, Russia	4	Swamp	82.0	55.5	26.86–26.88	61.40	0.00 to 15.00	1.97	54.47	6.76	0.00–0.13	*Glagolev et al.* [2011]
25	Auchencorth Moss, Edinburgh, Scotland, UK	72	Peat bog	−3.0	56.0	13.49	74.31	−18.10 to −8.10	0.90	41.65	4.40	−0.02–0.06	*Drewer et al.* [2010]
26	Forsinard, Scotland, UK	1	Peat bog	−4.0	58.5	14.71	90.50	−8.70	19.40	72.09	4.00	0.66	*Levy et al.* [2011]
27	Loch More, Caithness, Scotland, UK	21	Blanket bog	−3.5	58.5	20.93	90.50	−10.60 to −5.60	19.40	72.09	4.08	0.64–1.64	*MacDonald et al.* [1998]
28	Migneint A, Wales, UK	1	Blanket bog	−4.0	53.0	12.14	177.27	−10.10	5.20	54.81	4.30	0.70	*Levy et al.* [2011]
29	Migneint C, Wales, UK	1	Blanket bog	−4.0	53.0	18.36	177.27	−5.80	5.20	54.81	4.00	0.53	*Levy et al.* [2011]
30	Moor House, England, UK	15	Upland blanket peat	−2.5	54.5	11.19	100.01	−15.30 to −5.30	9.54	61.15	3.80	0.40–0.54	*Ward et al.* [2007]
31	Peaknaze B, Wales, UK	1	Upland grassland/mire	−2.0	53.5	12.55	94.01	−15.00	6.29	55.98	3.90	0.23	*Levy et al.* [2011]
32	Peaknaze C, Wales, UK	1	Upland grassland/mire	−2.0	53.5	12.68	94.01	−1.00	6.29	55.98	4.10	−0.01	*Levy et al.* [2011]
33	Tadham Moor, England, UK	1	Wetland meadow	−3.0	51.0	16.33	81.91	−32.70	0.85	44.29	6.40	−0.02	*Lloyd* [2006]
34	Whim, Edinburgh, Scotland, UK	1	Oligotrophic bog	−3.5	56.0	12.14	74.31	−2.60	0.90	41.65	3.60	0.92	*Sheppard et al.* [2004]

wetland CH_4 emissions at regional and global scales, and the estimated northern high-latitude wetland CH_4 budgets had a wide range of 20~157 Tg CH_4 yr^{-1}, with minimum and maximum reported by *Christensen et al*. [1996] and *Petrescu et al*. [2010], respectively.

[5] The uncertainty in these estimates could result from many sources including model structures, assumptions, parameterization, and choice of forcing data. Among these uncertainty sources, the paucity of CH_4 flux measurements could be an important factor. The lack of enough measurements of CH_4 fluxes and related environmental factors may limit the understanding of ecological processes in specific wetland ecosystems, the model assumptions, and the parameterization of models. All of these limit the abilities of process-based models to estimate wetland CH_4 emissions. In addition to the large uncertainty present in wetland CH_4 emissions, the sensitivity of CH_4 fluxes to environmental controls is not well understood, which also limits explicit representations of many mechanistic processes in models.

[6] Dramatic environmental changes including higher temperature, changes of precipitation pattern, thawing permafrost, and longer growing seasons all occur in the northern high latitudes compared with low latitudes [*Fedorov*, 1996; *Hansen et al*., 1996; *Romanovsky et al*., 2000]. Most of these environmental changes affect wetland CH_4 emissions, including the magnitude and temporal variations [*Friborg et al*., 1997; *Whalen and Reeburgh*, 1992; *Zimov et al*., 2006]. The complex interactions between climate, soil, and ecosystems in the northern high latitudes provide a significant challenge for CH_4 model studies. Without a sound understanding of all of these interactions, it is difficult to explicitly represent these interactions in process-based models.

[7] In view of these facts, we opt here to use an artificial neural network (ANN) to estimate wetland CH_4 emissions in the northern high latitudes. During the past decades, most of the field measurements of CH_4 fluxes were made in the northern high latitudes. With the accumulation of available flux measurements, there is an opportunity for using a data-driving ANN approach to estimate CH_4 emissions. The ANN approach has appeared as a great alternative to classical statistical models [*Delon et al*., 2007; *Dupont et al*., 2008], and it is particularly useful in quantifying the responses of nonlinear processes, like wetland CH_4 emissions. In this study, we first use the ANN approach to find the optimal nonlinear regression between CH_4 fluxes and key environmental controls. Driven with the spatially explicit data of climate, hydrology, and soil properties, the developed ANN is then extrapolated to the northern high latitudes (north of 45°N) to estimate wetland CH_4 emissions in this region.

2. Methods

2.1. Data Organization

[8] To begin, we collected direct CH_4 flux chamber measurements of wetland ecosystems in the northern high latitudes from peer-reviewed literature [e.g., *Glagolev et al*., 2011; *Levy et al*., 2011]. Our data contain CH_4 flux chamber measurements from 34 sites, covering a range of wetland types under various field conditions (Table 1 and Figure 1). Each site contains a collection of flux measurement records. These flux measurements were originally recorded as hourly,

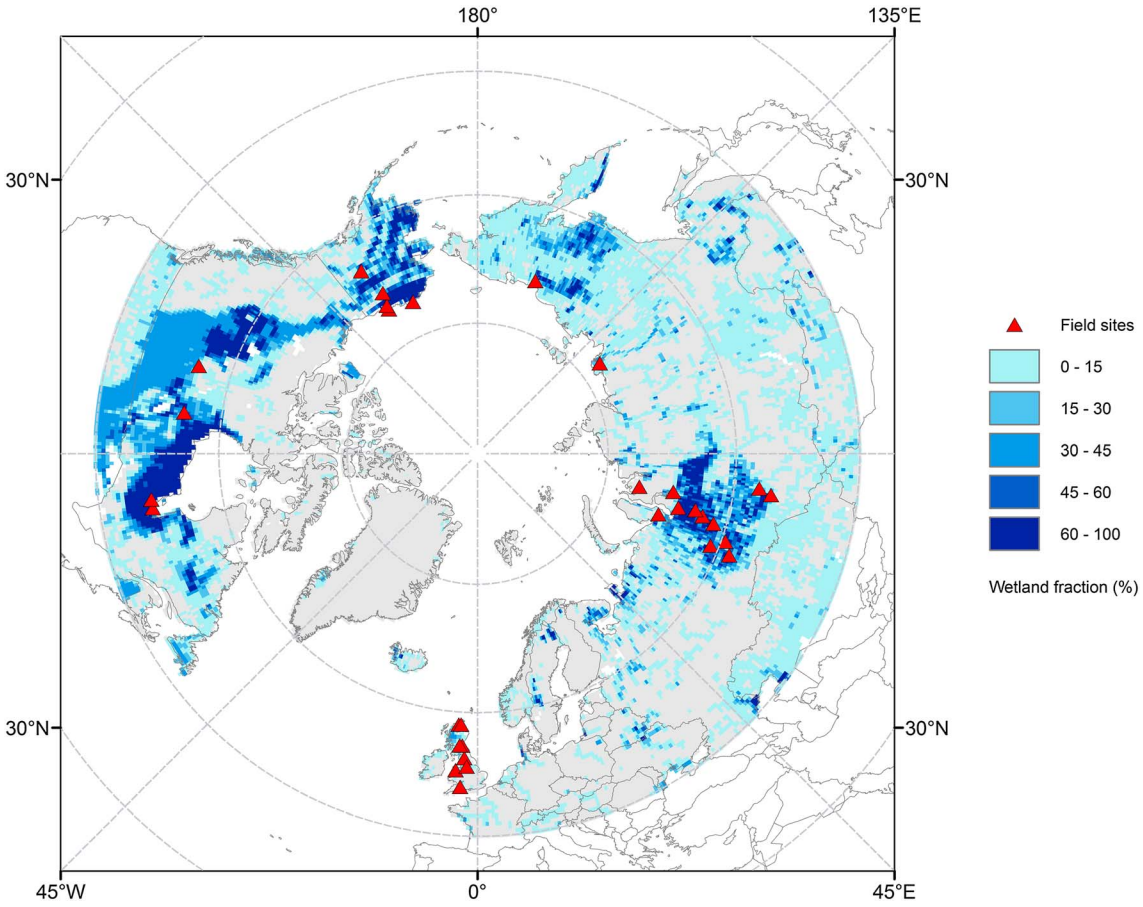

Figure 1. Spatial distribution of wetlands over the northern high latitudes (north of 45°N), overlaid by CH_4 flux observation sites used in this study. The fractional wetland areas are derived from the 30 s GLWD-3 wetland data set [*Lehner and Döll*, 2004].

daily, monthly, or growing-season flux values per unit wetland area. We converted them to monthly values in this study. Since most of original CH_4 flux measurements were hourly or daily values, we simply averaged all hourly or daily values within a month and aggregated to montly values for that month, without considering within-month flux variations. For those flux measurements recorded as growing-season flux values, at a few sites, we disaggregated evenly into monthly values without considering intermonth flux variations.

[9] The climate, hydrology, and soil property information we used included mean air temperature (T), precipitation (P), water table depth (WTD), soil organic carbon (SOC), soil total porosity (TP), and soil pH. These site-level data were first retrieved from original research papers and then complemented with other spatially explicit data sets based on the geographic coordinates and experiment dates of the measurements. Specifically, WTD data were entirely retrieved from original research papers. Complementary climate information was derived from a historical climate database (CRU TS3.1) from the Climate Research Unit (CRU) [*Mitchell and Jones*, 2005]. Complementary SOC, TP, and pH in the top soil (0–30 cm) were taken from the International Soil Reference and Information Centre World Inventory of Soil Emission Potentials (ISRIC-WISE) spatial soil database [*Batjes*, 2006]. The number of total measurement records for each variable is listed in Table 2. Only those having complete measurement records, containing both CH_4 fluxes and six environmental variables (N = 1049, due to the limited availability of WTD), were used for developing neural network models.

2.2. Neural Network Development

[10] The generalized regression neural network (GRNN) [*Specht*, 1991] was employed to perform the input-output mapping between the independent variables (six environmental variables) and the dependent variable (CH_4 fluxes). Similar to other kinds of neural networks, GRNN is a data-driven "black box" model. It can be used to estimate the

Table 2. Spearman Correlations Between CH_4 Flux Measurements (N = 1790) and Different Environmental Factors: Air Temperature (T), Precipitation (P), Water Table Depth (WTD), Soil Organic Carbon (SOC), Soil Total Porosity (TP), and Soil pH[a]

Parameter	T	P	WTD	SOC	TP	pH
N[b]	1552[c]	1790[d]	1049[c]	1790[d]	1790[d]	1072[c]
Coefficient	0.28	0.13	−0.25	0.17	0.17	0.07

[a]All values are statistically significant at the 1% level.
[b]Sample size of each pairwise correlation.
[c]Using observation data only.
[d]Derived from spatially explicit data sets.

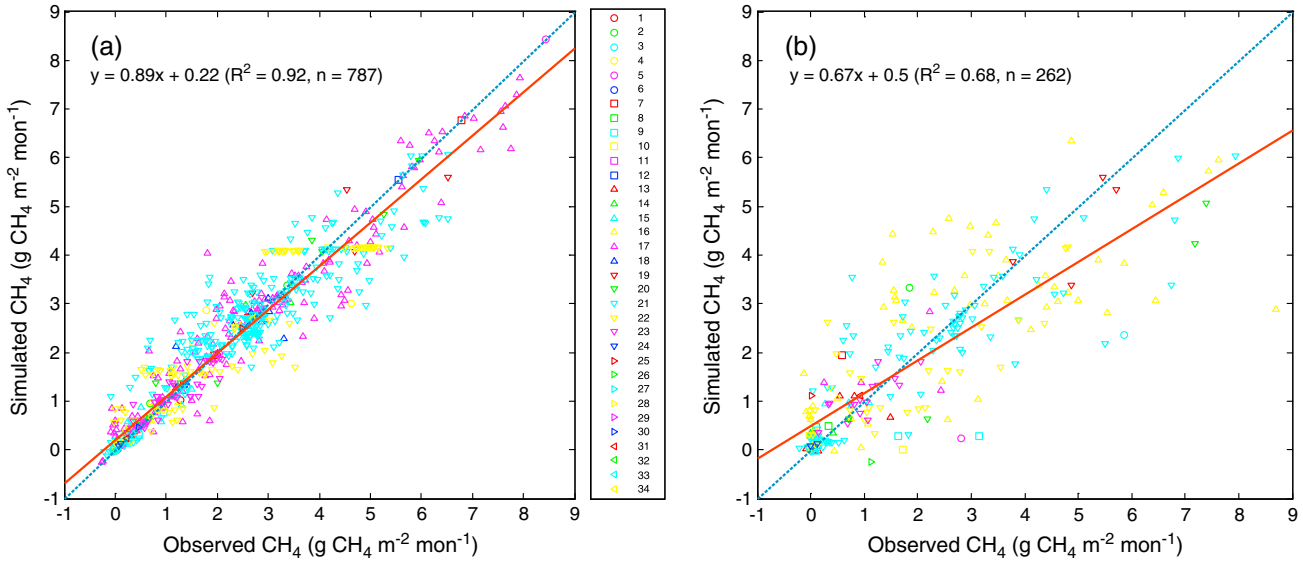

Figure 2. Comparisons between the measured and modeled monthly CH_4 emissions at all sites. (a) The ANN models were constructed based on the training data set, and (b) the validation data set was used to test the performance of the model. The dashed line is the 1:1 line, and the solid line is the fitted line. The site ID can be found in Table 1.

underlying nonlinear relationship between model inputs and outputs, requiring no prior knowledge of the inputs. Relative to other neural networks, GRNN has some advantages including fast learning (without an interative training procedure) and good convergence with a large number of training data [*Specht*, 1991]. Thus, the GRNN model is a suitable mathematical model to construct the relationship between CH_4 fluxes and the related environmental factors given that accurate prior knowledge (the link beween CH_4 emissions and environmental factors) is usually unavailable. The GRNN model has a four-layer network architecture consisting of input, pattern, summation, and output layers [*Zhuang et al*., 2012]. The training data set, including input and output values of measurements, is fed into this multilayer neural network, and the network is trained to obtain a set of optimized interconnected network weights which are used to produce the most probable value for the outputs. More details about the GRNN algorithm and network optimization method can be found in *Specht* [1991].

[11] In order to test the performance of the ANN model, the popular neural network validation method, train and test, was adopted to validate the capability of the developed model. Specifically, the whole measurement data set was randomly divided into two sets: a training set (75%; N = 787) used to construct the ANN model and a testing set (25%; N = 262) used to validate the constructed model. In addition, to compare the performance of the ANN model with those of traditional regression approaches, we also used a stepwise regression approach to model the relationship between monthly CH_4 fluxes and environmental variables based on the same training data set (see the supporting information). MATLAB codes were used for developing the ANN model (The Mathworks, 2006).

2.3. Regional Extrapolation

[12] The developed ANN model was used to simulate monthly CH_4 emissions from wetland ecosytems in the northern high latitudes from 1990 to 2009 at a 0.5° × 0.5° spatial resolution. In this study, we used the Global Lakes and Wetlands Database (GLWD) [*Lehner and Döll*, 2004] to define the spatial extent of wetland ecosystems in the northern high latitudes (north of 45°N). The cartography-based GLWD data set provides a global database of natural wetlands at a 30 s resolution (GLWD-3). We aggregated the 30 s GLWD-3 raster map to generate a data set of 0.5° × 0.5° resolution in which each 0.5° grid cell recorded the percentage of 30 s GLWD-3 wetland pixels.

[13] To extrapolate the ANN model, we organized spatially explicit climate, hydrology, and soil properties data. The climate data, including monthly air temperature and precipitation, were extracted from the CRU TS3.1 data sets [*Mitchell and Jones*, 2005]. The spatially explicit soil properties in the top soil (0–30 cm), including SOC, TP, and pH, were taken from the ISRIC-WISE spatial soil database [*Batjes*, 2006].

[14] The spatial extent of wetlands and the fractional wetland areas within each 0.5° grid cell were determined by the GLWD-3 data set [*Lehner and Döll*, 2004], while the WTD of wetlands within each 0.5° grid cell was derived from hydrological model simulations combined with a TOPMODEL-based method. The grid cell mean WTD was first simulated by a sophisticated hydrological model, which is able to simulate the soil moisture profile and WTD for wetland ecosystems [*Zhuang et al*., 2002, 2004]. Then we used the TOPMODEL-based formulation [*Lu and Zhuang*, 2012] to represent the spatially distributed WTD for each 1 km pixel within a 0.5° grid cell:

$$Z_{\mathrm{WTD}i} = Z_{\mathrm{WTD}} - f \times (k_i - \lambda) \quad (1)$$

where f is the decay parameter, k_i is the topographic wetness index (TWI), and λ is the average of k_i over a 0.5° grid cell. Z_{WTD} is the average WTD that is calculated from the hydrological model, and $Z_{\mathrm{WTD}i}$ is the local WTD at a 1 km spatial

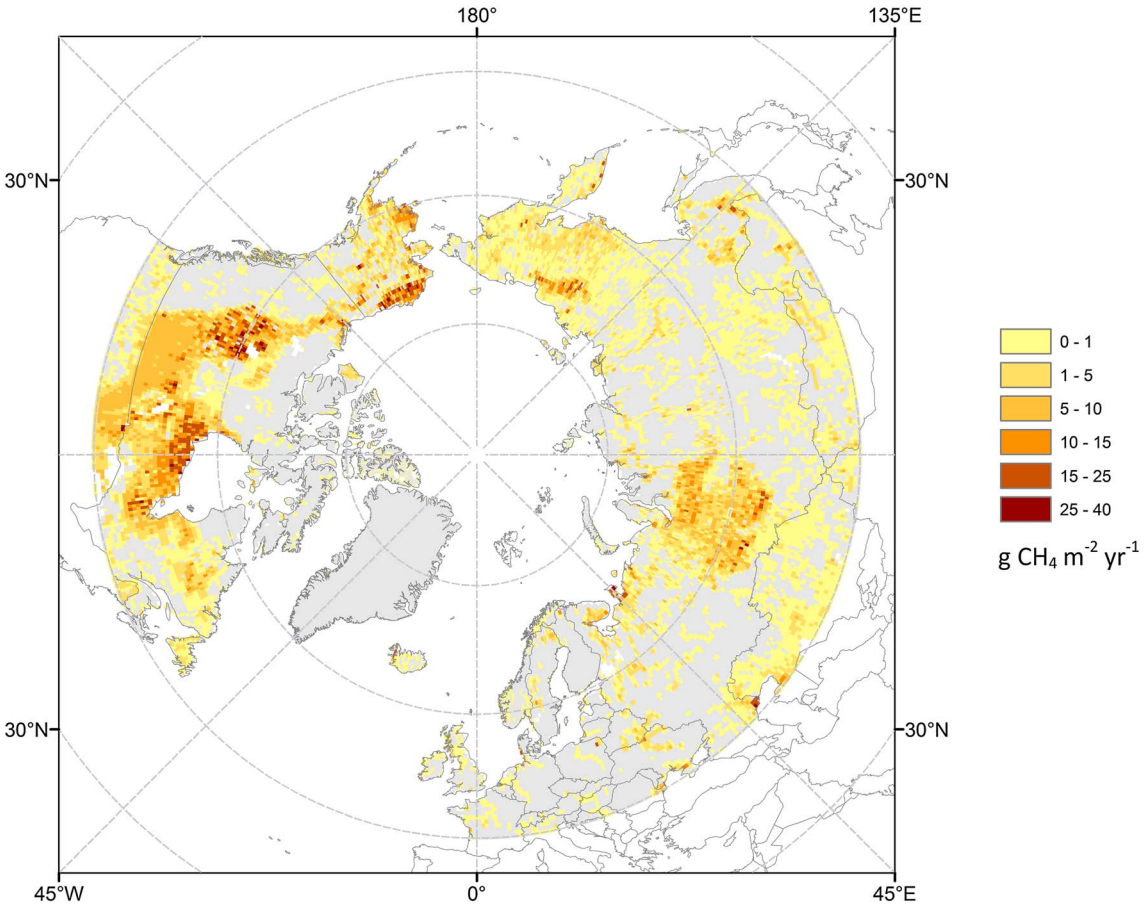

Figure 3. Grid cell mean wetland CH_4 emissions, averaged over 1990–2009, over the northern high latitudes (north of 45°N).

resolution. Following *Fan and Miguez-Macho* [2011], the decay parameter (f) was modeled as

$$f = \frac{100}{1 + 150 \times s} \times f_T \quad (f > 2.5\ \mathrm{m}) \tag{2}$$

$$f_T = 1.5 + 0.1 \times T \quad (-14^\circ\mathrm{C} < T < -5^\circ\mathrm{C}, f_T < 1) \tag{3}$$

$$f_T = 0.17 + 0.005 \times T \quad (T < -14^\circ\mathrm{C}, f_T \geq 0.05) \tag{4}$$

where s is the terrain slope and T is the mean surface air temperature in January. The 1 km topographic information and TWI were acquired from the HYDRO1k database (available on http://eros.usgs.gov/#Find_Data/Products_and_Data_Available/gtopo30/hydro), which provides comprehensive and consistent global coverage of topographically derived data based on the U.S. Geological Survey 30 s digital elevation model of the world (GTOPO30). After acquiring the local WTD (Z_{WTDi}) for each 1 km pixel within a 0.5° grid cell, we sorted Z_{WTDi} to get an ascending order of local WTD (Z_{WTDj}) and calculated the WTD of wetlands in that 0.5° grid cell (WTD_{wet}) as

$$WTD_{wet} = \frac{\sum_{j=1}^{j=n} Z_{WTDj}}{n} \tag{5}$$

where n is the number of 1 km wetland pixels within each 0.5° grid cell, and the value of n is determined by the multiplication of the number of 1 km pixels and the fraction of wetland pixels, derived from the GLWD-3 data set, within each grid cell.

2.4. Sensitivity and Uncertainty Analysis

[15] A regional inventory of wetland CH_4 emissions would typically have a wide range of emission estimates. Before exploring the uncertainty in model estimates, we first conducted a sensitivity analysis of the ANN model to reveal the sensitivities to each input data. We conducted 36 other regional simulations by altering the climate, hydrology, and soil input data uniformly for each grid cell at regional scale. Each of the six variables was individually increased or decreased at three levels: ±10%, ±25%, and ±50%. In each of these sensitivity simulations, when a single variable was changed, the other variables were held as the same as they were in the "baseline" simulation. The sensitivity was then calculated as the percentage change between the estimated mean CH_4 fluxes of each sensitivity and the baseline simulation.

[16] The uncertainty in our regional inventories of wetland CH_4 emissions is mainly due to uncertain regional forcing variables and model structures/parameters. Ideally, we should propagate uncertainties in these two kinds of sources to the model output. However, due to the lack of accurate prior knowledge of regional model inputs (the six environmental variables in this case), we excluded regional forcing uncertainty analysis by only focusing on the uncertainties associated with ANN model structures/parameters. The obtained ANN

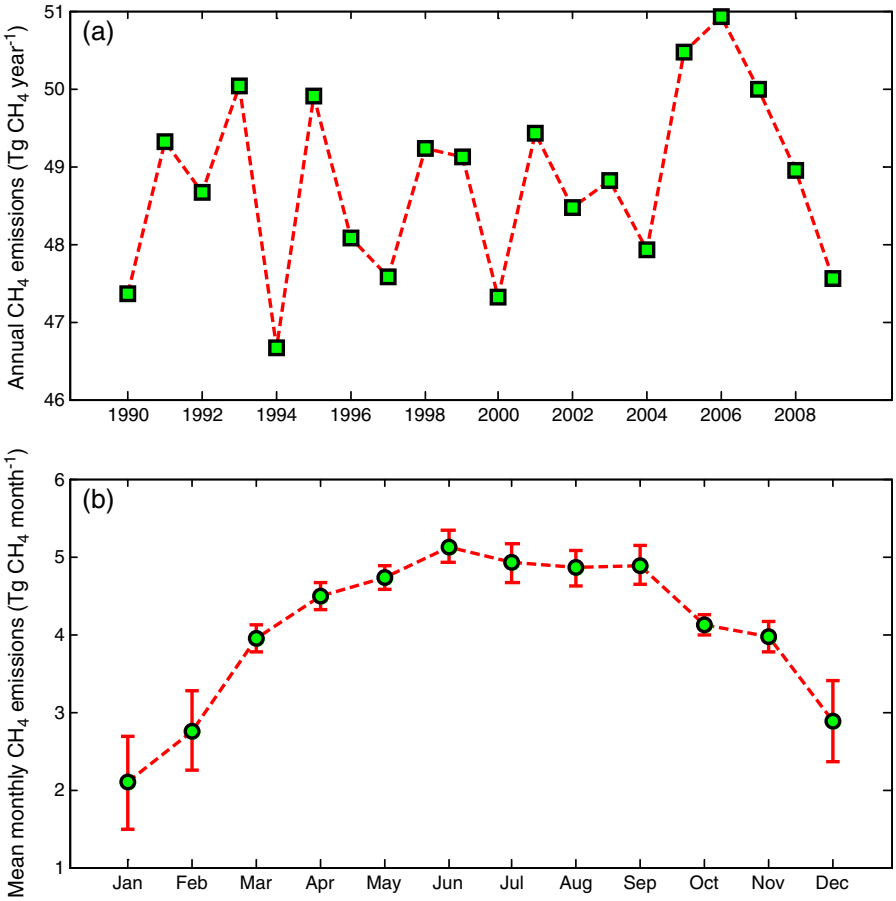

Figure 4. (a) Interannual and (b) seasonal variations of wetland CH_4 emissions from the northern high latitudes (north of 45°N). The error bars indicate one standard deviation of monthly emissions during 1990–2009.

model was a data-driven and highly nonlinear system with only optimized weight values; thus, it was difficult to directly quantify the uncertainty range of the model through parametric inference since the model parameters (or network weights) were determined on the basis of the training data set (subsampled from site measurements). Here the model uncertainty (structures/parameters) was assessed through developing a number of alternative models using the "delete-one" cross-validation method [*Zhuang et al.*, 2012]. Specifically, we randomly sampled three quarters of the training data from the organized measurement records to develop a new ANN model. Each possible training set was used to construct a different set of network parameters or weights, which was subsequently used for spatial extrapolation of CH_4 fluxes. During this step, the uncertainties in ANN model structures/parameters were quantified in an implicit manner. These steps were repeated 100 times to obtain 100 sets of regional estimates. The 95% confidence intervals of all estimates of CH_4 emissions were considered to be the range of model uncertainty and were thus used to define the lower and upper uncertainty bounds of the regional wetland CH_4 inventory.

3. Results

3.1. Artificial Neural Networks

[17] Before developing the ANN model, we first conducted a Spearman rank correlation analysis to explore the correlations between CH_4 flux measurements and other environmental factors. The pairwise correlation shows that CH_4 emissions are significantly correlated with climate, hydrology, and soil properties (Table 2). Among the six input variables, temperature and WTD are the two most important controls on CH_4 emissions. CH_4 emissions are correlated positively with air temperature and negatively with WTD (i.e., the lower the water table is, the less the CH_4 is emitted from wetland soils). There are also significant positive correlations between CH_4 emissions and SOC, soil total porosity, precipitation, and soil pH. Based on the correlation analysis, we found that these six environmental variables are all significantly correlated with wetland CH_4 fluxes, at a significance level of $p < 0.01$. Thus, we considered all these explanatory variables as the ANN model inputs.

[18] The simulated CH_4 fluxes from the ANN model are close to the observed data (root-mean-square error (RMSE) = 0.51 g CH_4 m^{-2} $month^{-1}$ for the training set and 1.1 g CH_4 m^{-2} $month^{-1}$ for the testing set), and the coefficients of determination (r^2) between the simulated and measured fluxes are 0.92 and 0.68 (at a significance level of $p < 0.01$) for the training set (Figure 2a) and the testing set (Figure 2b), respectively. The linear regression between the simulated and measured CH_4 fluxes is close to the 1:1 line, with some underestimation at higher fluxes for the testing set. In spite of the imperfect performance of the developed

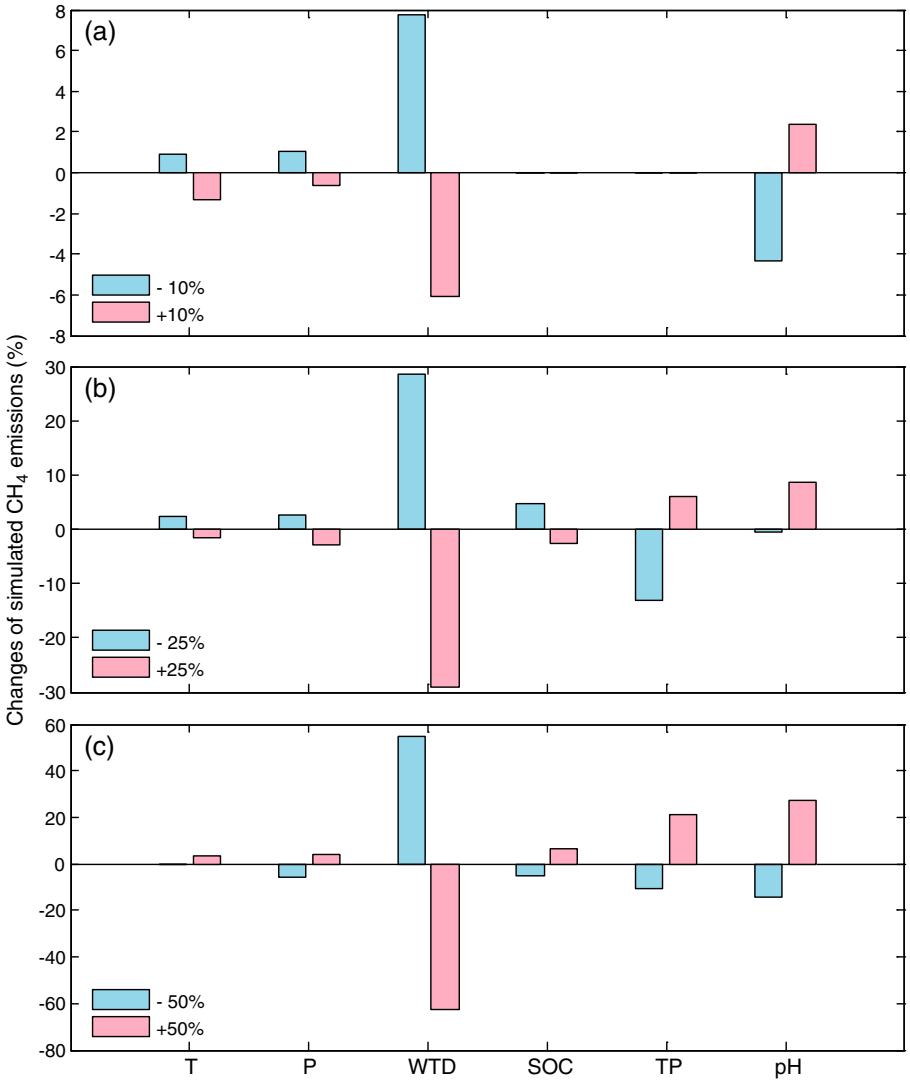

Figure 5. Sensitivity of the ANN model to changes in air temperature (*T*), precipitation (P), water table depth (WTD), soil organic carbon (SOC), soil total porosity (TP), and soil pH. The values are for the year 2000. The changes are calculated based on the baseline simulation using the unchanged regional input data.

ANN model, it is much better than the performance of the fitted stepwise regression model (Figure S1), which has a RMSE of 1.48 g CH_4 m^{-2} $month^{-1}$ with the same training data set ($r^2 = 0.43$).

3.2. Temporal Variations of Regional CH_4 Dynamics

[19] The CH_4 emissions from wetland ecosystems exhibit a large spatial variability over the northern high latitudes (Figure 3). The simulated emission patterns show that the Canadian lowlands, Alaska, West Siberia, and the far East Siberia are predominant sources of CH_4. The highest emissions of CH_4 occurred in two of the world's largest wetlands: the Hudson Bay Lowlands and the West Siberian Lowlands, where wetland ecosystems act as a source of atmospheric CH_4 up to 40 g CH_4 m^{-2} yr^{-1}.

[20] The annual wetland CH_4 fluxes show a significant interannual variability from 1990 to 2009 (Figure 4a). There is no significant trend of annual emissions during the period. The mean annual emissions are 48.8 Tg CH_4 yr^{-1}, with a range from 46.7 Tg CH_4 yr^{-1} in 1994 to 51.0 Tg CH_4 yr^{-1} in 2006. In terms of seasonal variability, wetland CH_4 emissions exhibit substantial seasonal variations with weak fluxes in the winter and strong fluxes in the summer (Figure 4b). The highest emissions of 5.1 Tg CH_4 $month^{-1}$ occurred in June while the lowest emissions of 2.1 Tg CH_4 $month^{-1}$ in January. The variations in monthly emissions during 1990–2009 are such that they are higher in the winter than in the summer.

3.3. Uncertainty of Regional CH_4 Estimates

[21] The sensitivity analysis of the ANN model was conducted by altering the input environmental variables individually (Figure 5). Among the six input variables, WTD stands out as the most sensitive one. Wetland CH_4 emissions change uniformly with WTD at three changing levels. Increasing WTD (lower water table) inhibits emissions, while decreasing WTD (higher water table) favors more emissions. Higher pH favors more emissions, while lower pH inhibits emissions. CH_4 emissions increase (decrease) with increasing (decreasing) TP at "medium"

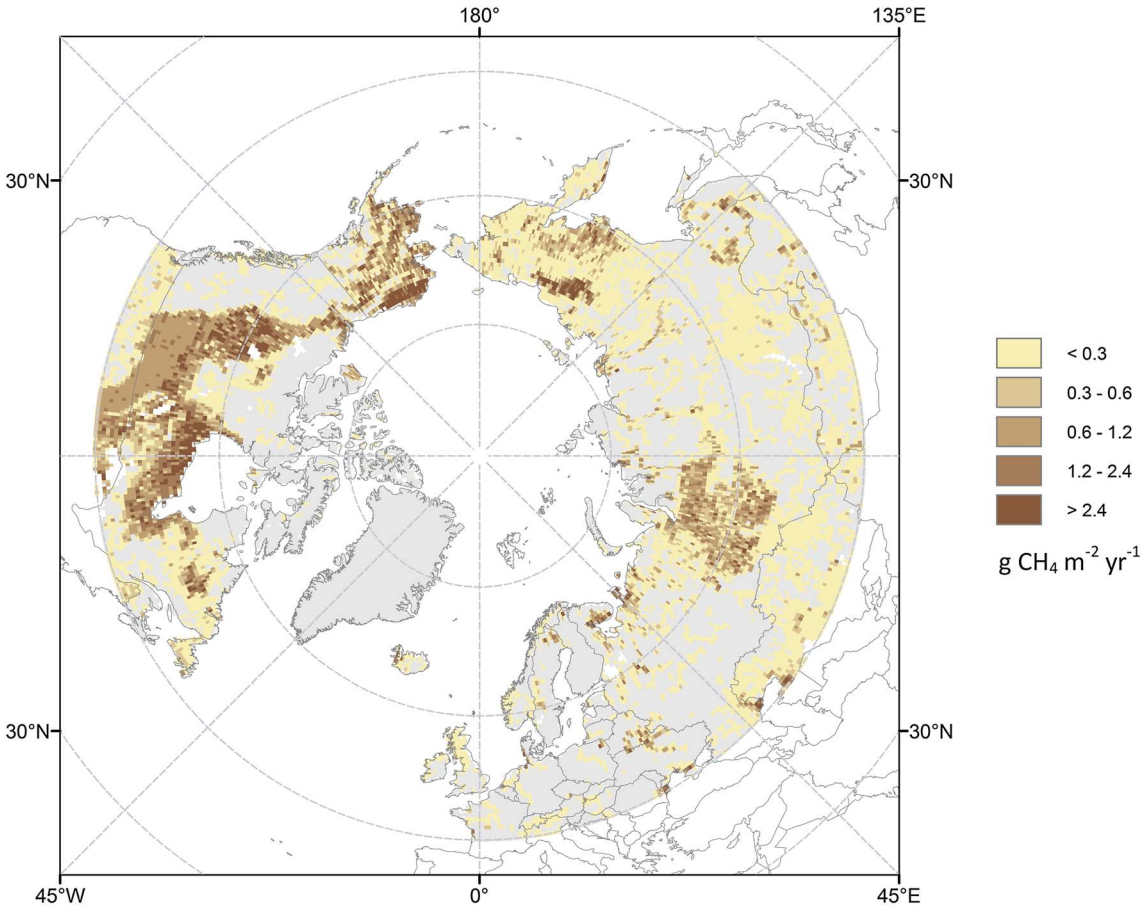

Figure 6. Standard deviation of annual wetland CH_4 emission rates for the year 2000, simulated with 100 ANN models.

and "large" levels, and there is no significant change of emissions at a "small" level. For the SOC and climate variables, no consistent relationship exists across the three changing levels.

[22] The uncertainty analyses of regional CH_4 emissions, based on 100 ANN models, indicate that larger uncertainties usually accompany higher CH_4 emission rates (Figures 3 and 6). The estimates of grid cell mean CH_4 fluxes from different ANN models do not vary significantly, with standard deviations normally lower than 2.4 g CH_4 m^{-2} yr^{-1}. The 100 ANN models provide a probability distribution of regional CH_4 emissions (Figure 7a). The uncertainties of regional CH_4 emissions from ANN model structures/parameters are defined, in our estimates, as the range between the lower bound and the upper bound of the 95% confidence intervals. There is little difference between the mean annual CH_4 emissions from the 100 ANN models (Figure 7b) and previous estimates (Figure 4a), but the interannual variability of annual CH_4 emissions increases once the model uncertainties are taken into account: The difference between the highest and lowest annual emissions changes from 4 to 14 Tg CH_4 yr^{-1} when the uncertainties are considered (Figures 4a and 7b). During the period of 1990–2009, the mean annual CH_4 emissions are 48.7 Tg CH_4 yr^{-1}, with the lower bound (44.0 Tg CH_4 yr^{-1}) and the upper bound (53.7 Tg CH_4 yr^{-1}) of the 95% confidence intervals.

4. Discussion

[23] In terms of correlation analyses, temperature condition and water availability strongly constrain CH_4 emissions from wetland soils. The high positive correlation between CH_4 fluxes and temperature is consistent with laboratory studies [e.g., *Whalen and Reeburgh*, 1996] and field observations [e.g., *Bellisario et al*., 1999; *Christensen et al*., 2003]. The correlation between the depth of the water table and CH_4 fluxes accords with field experiments [*Heikkinen et al*., 2002; *Nykänen et al*., 1998], suggesting that an inverse relationship exists between water table position and CH_4 fluxes (deeper water tables lead to smaller emissions). In addition, the heterogeneity of soil properties is also an important control on the variations of CH_4 emissions [*Levy et al*., 2011].

[24] Net CH_4 emissions from boreal wetland ecosystems have a wide range of estimates ranging from 20 Tg CH_4 yr^{-1} [*Christensen et al*., 1996] to 157 Tg CH_4 yr^{-1} [*Petrescu et al*., 2010] during the past decades, based on measurements or model simulations (Table 3). Our estimate of CH_4 emissions, 47~51 Tg CH_4 yr^{-1}, is within the range of these estimates and is comparable to the estimates from *Bartlett and Harriss* [1993] and *Zhuang et al*. [2004] focusing on the same region.

[25] Some anomalies in annual wetland CH_4 emissions can be identified during the period of 1990–2009, although no

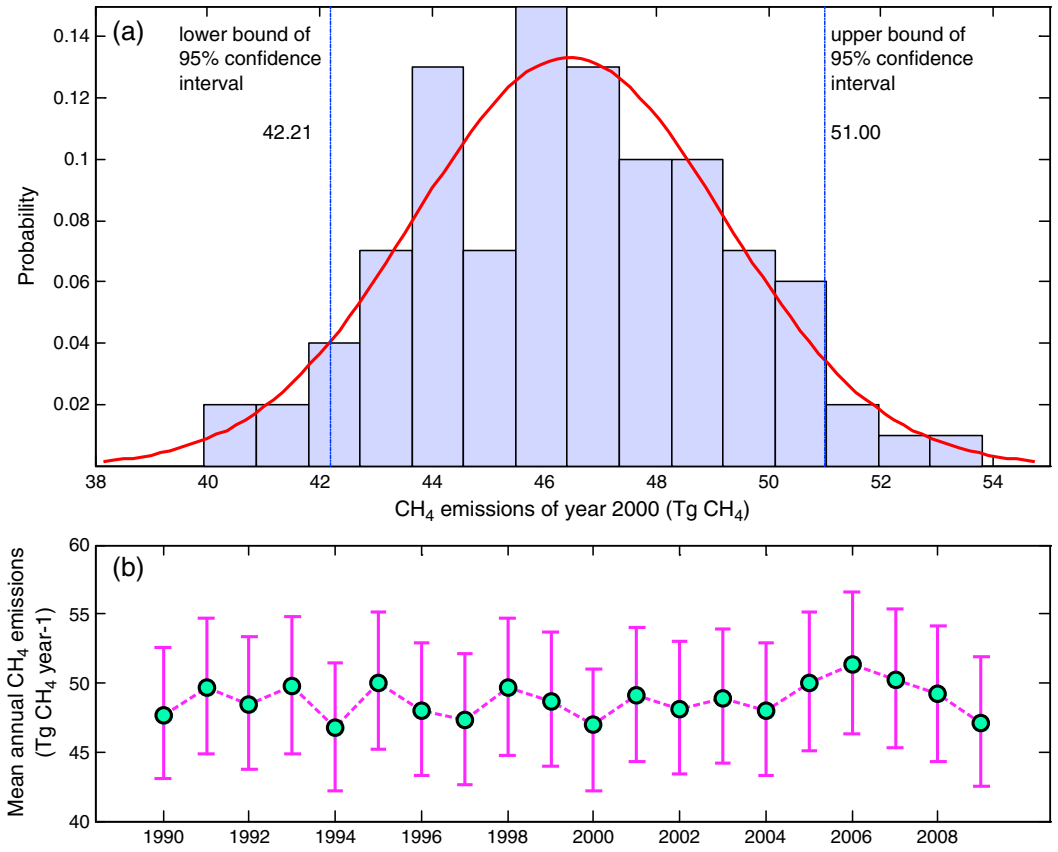

Figure 7. Uncertainties of the estimated wetland CH_4 emissions from the northern high latitudes (north of 45°N) with 100 ANN models: (a) probability distribution and the 95% confidence intervals of annual CH_4 emissions of year 2000 and (b) interannual variations of annual CH_4 emissions and the 95% confidence intervals from 1990 to 2009.

significant interannual trend exists. The CH_4 emissions in 1993 are higher than the emissions in 1992, which is the same as reported by *Bousquet et al.* [2006]. Consistent with many other studies [e.g., *Chen and Prinn*, 2006; *Mikaloff Fletcher et al.*, 2004], our estimates indicate a significant emission increase in 1998. Indeed, many previous studies [e.g., *Cunnold et al.*, 2002; *Dlugokencky et al.*, 2001] have attributed elevated CH_4 emissions in 1998 to strong El Niño phenomena which occurred in late 1997 and 1998 [*Bell et al.*, 1999] and influenced climate on a global scale. The higher emissions occurred in 2005 and 2006, which accords with the simulation results of *Petrescu et al.* [2010]. In addition, it is noted that the interannual variability of annual wetland CH_4 emissions increases when uncertainties of model structures/parameters are taken into account (Figures 4a and 7b).

[26] Sensitivity analyses indicate that the ANN model is more sensitive to the availability of water table and soil properties (e.g., pH and TP). WTD stands out as the most sensitive and consistent factor, suggesting that the water table position is the key control of CH_4 emissions. To date, most

Table 3. Emissions of CH_4 From Wetland Ecosystems in the Northern High Latitudes

Literature Sources	Emissions (Tg CH_4 yr^{-1})	Comments
Sebacher et al. [1986]	45–106	Estimates for Arctic and boreal wetlands
Matthews and Fung [1987]	62	Estimates for forested and nonforested bogs between 50°N and 70°N
Crill et al. [1988]	72	Estimates for undrained peatlands north of 40°N
Whalen and Reeburgh [1990]	53	Estimates for global tundra and taiga ecosystems
Fung et al. [1991]	35	Estimates for wetlands and tundra
Whalen and Reeburgh [1992]	42 ± 26	Estimates for Arctic wet meadow and tussock and shrub tundra
Bartlett and Harriss [1993]	38	Estimates for northern wetlands north of 45°N
Cao et al. [1996]	22	Estimates for natural wetlands north of 40°N
Christensen et al. [1996]	20 ± 13	Estimates for northern wetlands and tundra
Walter et al. [2001]	65	Estimates for wetlands north of 30°N
Zhuang et al. [2004]	57	Estimates for natural wetlands north of 45°N
Mikaloff Fletcher et al. [2004]	30–64	Estimates based on inverse modeling for boreal region
Chen and Prinn [2006]	34 ± 13	Estimates based on inverse modeling for boreal region wetlands
Petrescu et al. [2010]	38–157	Estimates for boreal and Arctic wetlands
This study	47–51	Estimates for natural wetlands north of 45°N

earth system models apply simplified representations of WTD, assuming an equally distributed water table in each grid cell without considering subgrid spatial heterogeneity when simulating wetland CH_4 emissions [*Petrescu et al*., 2010; *Walter et al*., 2001]. This simple representation of WTD neglects the effects of microtopography on water table dynamics, to which CH_4 production and oxidation processes are sensitive [*Zhuang et al*., 2007]. Although the developed ANN model could overfit the training data to a certain extent (Figure 2), the uncertainty analyses of model structures/parameters show little difference between the mean annual CH_4 emissions from the 100 ANN models and those from the optimized ANN model, which suggests that the structure of the optimized ANN model is well developed for estimating CH_4 emissions. Another uncertainty of the ANN model estimates could be from the spatial scale differences in models and their application since the ANN model was developed and parameterized at site level (from a few square meters to several kilometers) and applied to regional scale ($0.5° \times 0.5°$ in this case). In this study, we disregarded the differences in spatial scales by assuming that the relationships between CH_4 fluxes and environmental variables do not change across different spatial scales. But this assumption should be further assessed in future study.

[27] In addition to the uncertainties in the ANN model associated with CH_4 flux density (per unit wetland area), the extent of wetlands used for the estimates at regional scales could be an important source of uncertainty due to the difficulties in characterizing wetland areas and their dynamics [*Zhu et al*., 2011]. The regional total of CH_4 emissions may be greatly affected by the choice of wetland data set. For instance, a model study by *Petrescu et al*. [2010] gave a broad range of current CH_4 emissions, between 38 and 157 Tg CH_4 yr^{-1} from circum-Arctic wetlands ($< 5°C$ for mean annual air temperature) based on multiple different wetland extent data sets. In this study, we use the GLWD data set [*Lehner and Döll*, 2004] to define the spatial extent of wetlands, and we use a simulated monthly mean water table position of wetlands within a grid cell to represent hydrological dynamics of wetlands. The cartography-based GLWD data set is expected to represent the maximum extent of wetlands [*Lehner and Döll*, 2004], which may include the wetlands that are inundated only for a short time (or never inundated) over a year. In our simulations, we use fixed fractional wetland areas for each grid cell, without considering the expansion and contraction of wetland areas during the course of a year. Thus, our estimate of wetland CH_4 emissions could be higher than the actual value, especially for the winter months when contraction of wetland areas occurs. It would be better to utilize satellite-based wetland data sets [e.g., *Prigent et al*., 2007] to represent the temporal dynamics of wetland areas, but it should be kept in mind that satellites fail to detect those never inundated wetlands that are also associated with CH_4 emissions. Also, the choice of wetland extent data set influences the estimated WTD of wetlands within a grid cell, which is calculated from grid cell mean WTD and the fractional wetland area based on the TOPMODEL method (equations (1)–(5)).

5. Conclusions

[28] Based on published site-level CH_4 flux measurements of wetland ecosystems and associated environmental data, we develop a model to estimate wetland CH_4 emissions using an artificial neural network approach. The developed ANN model fits well with the observed CH_4 fluxes. The mean annual wetland CH_4 emissions in the northern high latitudes are estimated to be 48.7 Tg CH_4 yr^{-1} with an uncertainty range of 44.0~53.7 Tg CH_4 yr^{-1}, and there are both significant interannual and seasonal variations of emissions during the period of 1990–2009. We find that the regional wetland CH_4 emissions are most sensitive to variations in water table position. The simulated wetland CH_4 emissions show a large spatial variability over the northern high latitudes, due to variations in hydrology, climate, and soil conditions. To improve future assessments of wetland CH_4 dynamics in this region, research priorities should be directed to better characterizing hydrological dynamics of wetlands (i.e., variations of areas and water table position) in quantifying regional CH_4 emissions from northern wetlands.

[29] **Acknowledgments.** This study was supported through projects funded by the NASA Land-Cover/Land-Use Change Program (NASA-NNX09AI26G), the Department of Energy (DE-FG02-08ER64599), the NSF Division of Information and Intelligent Systems (NSF-1028291), and the NSF Carbon and Water in the Earth Program (NSF-0630319). Computing support was provided by the Rosen Center for Advanced Computing (RCAC) at Purdue University.

References

Andronova, N. G., and I. L. Karol (1993), The contribution of USSR sources to global methane emission, *Chemosphere*, *26*(1-4), 111–126.

Aselmann, I., and P. J. Crutzen (1989), Global distribution of natural freshwater wetlands and rice paddies, their net primary productivity, seasonality and possible methane emissions, *J. Atmos. Chem.*, *8*(4), 307–358.

Bartlett, K. B., and R. C. Harriss (1993), Review and assessment of methane emissions from wetlands, *Chemosphere*, *26*(1-4), 261–320.

Batjes, N. H. (2006), ISRIC-WISE derived soil properties on a 5 by 5 arc-minutes global grid (version 1.0), ISRIC—World Soil Inf., Wageningen, Netherlands.

Bell, G. D., M. S. Halpert, V. E. Kousky, M. E. Gelman, C. F. Ropelewski, A. V. Douglas, and R. C. Schnell (1999), Climate assessment for 1998, *Bull. Am. Meteorol. Soc.*, *80*(5), 1040–1040.

Bellisario, L. M., J. L. Bubier, T. R. Moore, and J. P. Chanton (1999), Controls on CH_4 emissions from a northern peatland, *Global Biogeochem. Cycles*, *13*(1), 81–91.

Bousquet, P., et al. (2006), Contribution of anthropogenic and natural sources to atmospheric methane variability, *Nature*, *443*(7110), 439–443.

Cao, M., S. Marshall, and K. Gregson (1996), Global carbon exchange and methane emissions from natural wetlands: Application of a process-based model, *J. Geophys. Res.*, *101*(D9), 14,399–14,414.

Chen, Y. H., and R. G. Prinn (2006), Estimation of atmospheric methane emissions between 1996 and 2001 using a three-dimensional global chemical transport model, *J. Geophys. Res.*, *111*, D10307, doi:10.1029/2005JD006058.

Christensen, T. R. (1993), Methane emission from Arctic tundra, *Biogeochemistry*, *21*(2), 117–139.

Christensen, T. R., S. Jonasson, T. V. Callaghan, and M. Havström (1995), Spatial variation in high-latitude methane flux along a transect across Siberian and European tundra environments, *J. Geophys. Res.*, *100*(D10), 21,035–21,021.

Christensen, T. R., I. C. Prentice, J. Kaplan, A. Haxeltine, and S. Sitch (1996), Methane flux from northern wetlands and tundra, *Tellus, Ser. B*, *48*(5), 652–661.

Christensen, T. R., A. Ekberg, L. Strom, M. Mastepanov, N. Panikov, M. Oquist, B. H. Svensson, H. Nykanen, P. J. Martikainen, and H. Oskarsson (2003), Factors controlling large scale variations in methane emissions from wetlands, *Geophys. Res. Lett.*, *30*(7), 1414, doi:10.1029/2002GL016848.

Crill, P. M., K. B. Bartlett, R. C. Harriss, E. Gorham, E. S. Verry, D. I. Sebacher, L. Madzar, and W. Sanner (1988), Methane flux from Minnesota peatlands, *Global Biogeochem. Cycles*, *2*(4), 371–384.

Cunnold, D. M., et al. (2002), In situ measurements of atmospheric methane at GAGE/AGAGE sites during 1985–2000 and resulting source inferences, *J. Geophys. Res.*, *107*(D14), 4225, doi:10.1029/2001JD001226.

Delon, C., D. SerCa, C. Boissard, R. Dupont, A. Dutot, P. Laville, P. de Rosnay, and R. Delmas (2007), Soil NO emissions modelling using artificial neural network, *Tellus, Ser. B*, *59*(3), 502–513.

Dlugokencky, E. J., B. P. Walter, K. A. Masarie, P. M. Lang, and E. S. Kasischke (2001), Measurements of an anomalous global methane increase during 1998, *Geophys. Res. Lett.*, *28*(3), 499–502.

Dlugokencky, E. J., L. Bruhwiler, J. W. C. White, L. K. Emmons, P. C. Novelli, S. A. Montzka, K. A. Masarie, P. M. Lang, A. M. Crotwell, and J. B. Miller (2009), Observational constraints on recent increases in the atmospheric CH_4 burden, *Geophys. Res. Lett.*, *36*, L18803, doi:10.1029/2009GL039780.

Drewer, J., A. Lohila, M. Aurela, T. Laurila, K. Minkkinen, T. Penttilä, K. J. Dinsmore, R. M. McKenzie, C. Helfter, and C. Flechard (2010), Comparison of greenhouse gas fluxes and nitrogen budgets from an ombotrophic bog in Scotland and a minerotrophic sedge fen in Finland, *Eur. J. Soil Sci.*, *61*(5), 640–650.

Dupont, R., K. Butterbach-Bahl, C. Delon, N. Bruggemann, and D. Serça (2008), Neural network treatment of 4 years long NO measurement in temperate spruce and beech forests, *J. Geophys. Res.*, *113*, G04001, doi:10.1029/2007JG000665.

Fan, Y., and G. Miguez-Macho (2011), A simple hydrologic framework for simulating wetlands in climate and earth system models, *Clim. Dyn.*, *37*(1), 253–278.

Fedorov, A. N. (1996), Effects of recent climate change on permafrost landscapes in central Sakha, *Polar Geogr.*, *20*(2), 99–108.

Friborg, T., T. R. Christensen, and H. Søgaard (1997), Rapid response of greenhouse gas emission to early spring thaw in a subarctic mire as shown by micrometeorological techniques, *Geophys. Res. Lett.*, *24*(23), 3061–3064.

Fung, I., M. Prather, J. John, J. Lerner, and E. Matthews (1991), Three-dimensional model synthesis of the global methane cycle, *J. Geophys. Res.*, *96*(D7), 13,033–13,065.

Glagolev, M., I. Kleptsova, I. Filippov, S. Maksyutov, and T. Machida (2011), Regional methane emission from West Siberia mire landscapes, *Environ. Res. Lett.*, *6*, 045214, doi:10.1088/1748-9326/6/4/045214.

Granberg, G., C. Mikkelä, I. Sundh, B. H. Svensson, and M. Nilsson (1997), Sources of spatial variation in methane emission from mires in northern Sweden: A mechanistic approach in statistical modeling, *Global Biogeochem. Cycles*, *11*(2), 135–150.

Hansen, J., R. Ruedy, M. Sato, and R. Reynolds (1996), Global surface air temperature in 1995: Return to pre Pinatubo level, *Geophys. Res. Lett.*, *23*(13), 1665–1668.

Hanson, R. S., and T. E. Hanson (1996), Methanotrophic bacteria, *Microbiol. Mol. Biol. Rev.*, *60*(2), 439–471.

Heikkinen, J. E. P., V. Elsakov, and P. J. Martikainen (2002), Carbon dioxide and methane dynamics and annual carbon balance in tundra wetland in NE Europe, Russia, *Global Biogeochem. Cycles*, *16*(4), 1115, doi:10.1029/2002GB001930.

Heyer, J., U. Berger, I. L. Kuzin, and O. N. Yakovlev (2002), Methane emissions from different ecosystem structures of the subarctic tundra in Western Siberia during midsummer and during the thawing period, *Tellus, Ser. B*, *54*(3), 231–249.

Lehner, B., and P. Döll (2004), Development and validation of a global database of lakes, reservoirs and wetlands, *J. Hydrol.*, *296*(1–4), 1–22.

Levy, P. E., A. Burden, M. D. A. Cooper, K. J. Dinsmore, J. Drewer, C. Evans, D. Fowler, J. Gaiawyn, A. Gray, and S. K. Jones (2011), Methane emissions from soils: Synthesis and analysis of a large UK data set, *Global Change Biol.*, *18*(5), 1657–1669.

Lloyd, C. R. (2006), Annual carbon balance of a managed wetland meadow in the Somerset Levels, UK, *Agric. For. Meteorol.*, *138*(1–4), 168–179.

Lu, X., and Q. Zhuang (2012), Modeling methane emissions from the Alaskan Yukon River basin, 1986–2005, by coupling a large-scale hydrological model and a process-based methane model, *J. Geophys. Res.*, *117*, G02010, doi:10.1029/2011JG001843.

MacDonald, J. A., D. Fowler, K. J. Hargreaves, U. Skiba, I. D. Leith, and M. B. Murray (1998), Methane emission rates from a northern wetland; response to temperature, water table and transport, *Atmos. Environ.*, *32*(19), 3219–3227.

Matthews, E., and I. Fung (1987), Methane emission from natural wetlands: Global distribution, area, and environmental characteristics of sources, *Global Biogeochem. Cycles*, *1*(1), 61–86.

Mikaloff Fletcher, S. E., P. P. Tans, L. M. Bruhwiler, J. B. Miller, and M. Heimann (2004), CH_4 sources estimated from atmospheric observations of CH_4 and its $^{13}C/^{12}C$ isotopic ratios: 2. Inverse modeling of CH_4 fluxes from geographical regions, *Global Biogeochem. Cycles*, *18*, GB4005, doi:10.1029/2004GB002224.

Mitchell, T. D., and P. D. Jones (2005), An improved method of constructing a database of monthly climate observations and associated high-resolution grids, *Int. J. Climatol.*, *25*(6), 693–712.

Moore, T. R., A. Heyes, and N. T. Roulet (1994), Methane emissions from wetlands, southern Hudson Bay Lowland, *J. Geophys. Res.*, *99*(D1), 1455–1467.

Moosavi, S. C., P. M. Crill, E. R. Pullman, D. W. Funk, and K. M. Peterson (1996), Controls on CH_4 flux from an Alaskan boreal wetland, *Global Biogeochem. Cycles*, *10*(2), 287–296.

Nakano, T., S. Kuniyoshi, and M. Fukuda (2000), Temporal variation in methane emission from tundra wetlands in a permafrost area, northeastern Siberia, *Atmos. Environ.*, *34*(8), 1205–1213.

Nykänen, H., J. Alm, J. Silvola, K. Tolonen, and P. J. Martikainen (1998), Methane fluxes on boreal peatlands of different fertility and the effect of long-term experimental lowering of the water table on flux rates, *Global Biogeochem. Cycles*, *12*(1), 53–69.

O'Connor, F. M., et al. (2010), Possible role of wetlands, permafrost, and methane hydrates in the methane cycle under future climate change: A review, *Rev. Geophys.*, *48*, RG4005, doi:10.1029/2010RG000326.

Petrescu, A. M. R., L. P. H. van Beek, J. van Huissteden, C. Prigent, T. Sachs, C. A. R. Corradi, F. J. W. Parmentier, and A. J. Dolman (2010), Modeling regional to global CH4 emissions of boreal and Arctic wetlands, *Global Biogeochem. Cycles*, *24*, GB4009, doi:10.1029/2009GB003610.

Prigent, C., F. Papa, F. Aires, W. B. Rossow, and E. Matthews (2007), Global inundation dynamics inferred from multiple satellite observations, 1993–2000, *J. Geophys. Res.*, *112*, D12107, doi:10.1029/2006JD007847.

Rhew, R. C., Y. A. Teh, and T. Abel (2007), Methyl halide and methane fluxes in the northern Alaskan coastal tundra, *J. Geophys. Res.*, *112*, G02009, doi:10.1029/2006JG000314.

Romanovsky, V. E., T. E. Osterkamp, T. S. Sazonova, N. I. Shender, and V. T. Balobaev (2000), Past and future changes in permafrost temperatures along the East Siberian Transect and an Alaskan Transect, *Eos. Trans. AGU*, *81*(48), Fall Meet. Suppl., Abstract B71F-09.

Sachs, T., M. Giebels, J. Boike, and L. Kutzbach (2010), Environmental controls on CH_4 emission from polygonal tundra on the microsite scale in the Lena river delta, Siberia, *Global Change Biol.*, *16*(11), 3096–3110.

Sebacher, D. I., R. C. Harriss, K. B. Bartlett, S. M. Sebacher, and S. S. Grice (1986), Atmospheric methane sources: Alaskan tundra bogs, an alpine fen, and a subarctic boreal marsh, *Tellus, Ser. B*, *38*(1), 1–10.

Sheppard, L. J., A. Crossley, I. D. Leith, K. J. Hargreaves, J. A. Carfrae, N. Van Dijk, J. N. Cape, D. Sleep, D. Fowler, and J. A. Raven (2004), An automated wet deposition system to compare the effects of reduced and oxidised N on ombrotrophic bog species: Practical considerations, *Water Air Soil Pollut. Focus*, *4*(6), 197–205.

Solomon, S., D. Qin, M. Manning, Z. Chen, M. Marquis, K. B. Averyt, M. Tignor, and H. L. Miller (2007), *Change 2007: The Physical Science Basis: Working Group I Contribution to the Fourth Assessment Report of the IPCC*, Cambridge Univ. Press, Cambridge, U. K.

Specht, D. F. (1991), A general regression neural network, *IEEE Trans. Neural Networks*, *2*(6), 568–576.

Turetsky, M. R., R. K. Wieder, and D. H. Vitt (2002), Boreal peatland C fluxes under varying permafrost regimes, *Soil Biol. Biochem.*, *34*(7), 907–912.

Vourlitis, G. L., W. C. Oechel, S. J. Hastings, and M. A. Jenkins (1993), A system for measuring in situ CO_2 and CH_4 flux in unmanaged ecosystems: An Arctic example, *Funct. Ecol.*, *7*(3), 369–379.

Wagner, D., A. Lipski, A. Embacher, and A. Gattinger (2005), Methane fluxes in permafrost habitats of the Lena Delta: Effects of microbial community structure and organic matter quality, *Environ. Microbiol.*, *7*(10), 1582–1592.

Walter, B. P., M. Heimann, and E. Matthews (2001), Modeling modern methane emissions from natural wetlands 1. Model description and results, *J. Geophys. Res.*, *106*(D24), 34,189–34,206.

Ward, S. E., R. D. Bardgett, N. P. McNamara, J. K. Adamson, and N. J. Ostle (2007), Long-term consequences of grazing and burning on northern peatland carbon dynamics, *Ecosystems*, *10*(7), 1069–1083.

Whalen, S. C., and W. S. Reeburgh (1990), Consumption of atmospheric methane by tundra soils, *Nature*, *346*, 160–162.

Whalen, S. C., and W. S. Reeburgh (1992), Interannual variations in tundra methane emission: A 4-year time series at fixed sites, *Global Biogeochem. Cycles*, *6*(2), 139–159.

Whalen, S. C., and W. S. Reeburgh (1996), Moisture and temperature sensitivity of CH_4 oxidation in boreal soils, *Soil Biol. Biochem.*, *28*(10–11), 1271–1281.

Whitman, W. B., T. L. Bowen, and D. R. Boone (1992), The methanogenic bacteria, in *The Prokaryotes, a Handbook on the Biology of Bacteria: Ecophysiology, Isolation, Identification, Applications*, 2nd ed. Springer-Verlag, New York.

Wuebbles, D. J., and K. Hayhoe (2002), Atmospheric methane and global change, *Earth Sci. Rev.*, *57*(3–4), 177–210.

Zhu, X., Q. Zhuang, M. Chen, A. Sirin, J. Melillo, D. Kicklighter, A. Sokolov, and L. Song (2011), Rising methane emissions in response

to climate change in Northern Eurasia during the 21st century, *Environ. Res. Lett.*, *6*, 045211, doi:10.1088/1748-9326/6/4/045211.

Zhuang, Q., A. D. McGuire, K. P. O'Neill, J. W. Harden, V. E. Romanovsky, and J. Yarie (2002), Modeling soil thermal and carbon dynamics of a fire chronosequence in interior Alaska, *J. Geophys. Res.*, *107*(D1), 8147, doi:10.1029/2001JD001244.

Zhuang, Q., J. M. Melillo, D. W. Kicklighter, R. G. Prinn, A. D. McGuire, P. A. Steudler, B. S. Felzer, and S. Hu (2004), Methane fluxes between terrestrial ecosystems and the atmosphere at northern high latitudes during the past century: A retrospective analysis with a process-based biogeochemistry model, *Global Biogeochem. Cycles*, *18*, GB3010, doi:10.1029/2004GB002239.

Zhuang, Q., J. M. Melillo, A. D. McGuire, D. W. Kicklighter, R. G. Prinn, P. A. Steudler, B. S. Felzer, and S. Hu (2007), Net emissions of CH_4 and CO_2 in Alaska: Implications for the region's greenhouse gas budget, *Ecol. Appl.*, *17*(1), 203–212.

Zhuang, Q., Y. Lu, and M. Chen (2012), An inventory of global N_2O emissions from the soils of natural terrestrial ecosystems, *Atmos. Environ.*, *47*, 66–75.

Zimov, S. A., E. A. G. Schuur, and F. S. Chapin Iii (2006), Permafrost and the global carbon budget, *Science*, *312*, 1612–1613.